J. Phys. Chem. A **2004,** *108,* 3865−3872

Reliable Theoretical Procedures for the Calculation of Electronic-Structure Information in Hydrogen Abstraction Reactions

Michelle L. Coote*

Research School of Chemistry, Australian National University, Canberra, ACT 0200, Australia

Received: January 11, 2004; In Final Form: March 2, 2004

Geometries, barriers, and enthalpies have been calculated at a variety of levels of theory for a test set of seven H-atom abstraction reactions: $CH_2X\bullet + CH_3Y \rightarrow CH_3X + CH_2Y\bullet$ for (X,Y) = (H,H), (F,H), (Li,H), (Li,F), (CN,H), (OH,H), and (OH,CN). The objective was to select reliable yet cost-effective theoretical procedures for studying H-atom abstraction reactions that involve carbon-centered radicals, to facilitate the study of these reactions in biological and polymerization applications. To this end, geometry optimizations have been observed to be relatively insensitive to the level of theory, although the Hartree-Fock (HF) and Möller-Plesset second-order perturbation (MP2) methods should be avoided for spin-contaminated systems. The QCISD/6-31G(d) method provided excellent agreement with CCSD(T)/6-311G(d,p) and would provide a suitable benchmark level of theory when the latter could not be afforded, whereas MPW1K/6-31+G(d,p) provided excellent low-cost performance and would thus be suitable for larger systems. Barriers and enthalpies were more sensitive to the level of theory; nonetheless, the various high-level composite procedures (including the G3, G3-RAD, CBS, and W1 families of methods) were generally in excellent agreement with each other. However, in the spin-contaminated reactions, the spin-correction term in the CBS-QB3 procedure seems to be introducing a systematic error and may require some adjustment. The MPW1K/6-311+G(3df,2p) method provided excellent low-cost performance, and would be suitable for larger systems, whereas the RMP2/6-311+G(3df,2p) method also performed well, especially for predicting the reaction enthalpies and other thermochemical properties.

1. Introduction

H-atom abstraction between carbon-centered radicals has an important role in a variety of chemical and biochemical processes. For example, in free-radical polymerization, the propagating polymeric radical can undergo a variety of intermolecular and intramolecular hydrogen abstraction reactions, which affect the molecular weight and architecture of the resulting polymer. In the biological field, H-atom abstraction by the adenosyl radical is the key activation step in co-enzyme B-12 mediated processes such as diol dehydratase, whereas H-atom abstraction reactions that involve polypeptide radicals are associated with various physiological disorders such as arteriosclerosis and Alzheimer's disease. The calculation of electronic-structure information for these reactions provides an important tool for understanding their mechanisms. However, it is important to identify reliable yet cost-effective theoretical procedures that can be applied to the (typically large) systems that are relevant to biological and polymerization processes.

The development of composite ab initio procedures, such as the G3,[1] G3-RAD,[2] CBS,[3] and Wn[4] families of methods, has provided access to accurate electronic structure properties, at a fraction of the cost of the corresponding "pure" ab initio methods. The composite procedures accomplish this feat by approximating CCSD(T) or QCISD(T) energies with a large or infinite basis set, using additivity and/or extrapolation corrections. Depending on the procedure, various additional corrections (such as corrections for spin−orbit coupling) are also incorporated. When assessed against large tests sets of experimental thermochemical data (such as atomization energies, heats of formation, ionization potentials, and electron affinities), these procedures have been found to display "chemical accuracy"—showing deviations from experiment on the order of 1−2 kJ/mol for the highest-level procedures (such as W1 and W2),[4] and 4−8 kJ/mol for the lower-cost G3 and CBS procedures.[3,5]

The systematic comparison of the performance of the alternative high-level procedures (i.e., the CBS, G3, G3-RAD, and Wn methods) does not seem to have been performed on any large scale for hydrogen abstraction reactions. However, there have been many isolated studies, which indicate that composite methods may provide accurate barriers for such reactions. For example, the use of CCSD(T) energies with a large basis set was shown to reproduce the experimental barriers and enthalpies of 22 hydrogen abstraction reactions within ∼6 kJ/mol.[6] This effectively represents an unextrapolated version of the Wn methods, and, thus, one might expect even better results from the Wn methods themselves. Another large study found that the CBS-APNO method reproduced experimental barriers for hydrogen abstraction reactions to within 4 kJ/mol.[7] The same study noted that the errors in the barriers at the G2 level of theory were much larger (12 kJ/mol) but were considerably reduced for reaction enthalpies. Moreover, the RAD variants of G3 have been shown to provide excellent estimates of radical stabilization energies[8] and, hence, should be expected to provide excellent hydrogen abstraction enthalpies. It would therefore be of interest to compare the performance of the G3-RAD and also the latest non-RAD G3 methods for studying hydrogen abstraction reactions, with that of the CBS procedures, and also the higher-level Wn methods. Such a

---

* Author to whom correspondence should be addressed. E-mail address: mcoote@rsc.anu.edu.au.

10.1021/jp049863v CCC: $27.50

comparison would be of particular interest, because it has recently been noted that the (empirically based) spin-contamination correction term in the CBS procedures seems to be introducing a systematic error in the calculations of other radical reactions, such as the addition to multiple bonds[9,10] and N−H bond dissociation energies.[11]

When high-level composite procedures cannot be afforded, hybrid density functional theory (DFT) methods, such as B3-LYP, are usually adopted. These methods frequently offer access to accurate structural and thermochemical properties for stable molecules, at a fraction of the computational cost of ab initio methods of comparable accuracy.[12] However, they often show considerable errors for barrier heights and transition-state geometries. For example, in radical addition to C═S bonds, the popular hybrid DFT method B3-LYP significantly overestimates the forming bond lengths in the transition structures and underestimates the reaction barriers.[9] In fact, for these reactions, the B3-LYP method also shows considerable errors in the reaction enthalpies as well.[9] The failure of B3-LYP for calculating the barrier heights in hydrogen abstraction reactions is also well-documented,[6,7,13−16] and mean absolute errors of 13−17 kJ/mol and maximum errors of over 30 kJ/mol have been reported when the method is assessed against large test sets of experimental barrier heights.[6,7,13] Interestingly, it has been noted that the largest errors in the B3-LYP method often occur when polar effects are significant,[14,15] and this trend has also been noted in radical addition reactions[16] and in R−X bond dissociation energies (BDEs).[17] In this latter case, the B3-LYP method even fails to reproduce the correct qualitative ordering of the BDEs for the series R = Me, Et, *i*-Pr, and *t*-Bu, when X is an electronegative substituent (such as OH or OCH_3).[17] This result suggests that, for polar hydrogen abstraction reactions, the B3-LYP method may show considerable errors for the enthalpies (which are the difference of two BDEs), as well as for the barriers.

To provide improved low-cost performance for calculating barrier heights, two new hybrid DFT methods—MPW1K[6,13,18] and KMLYP[7]—have recently been designed. For specific details on these new methods, the reader is referred to the original references. However, note that one important difference between these methods and B3-LYP is the inclusion of a greater proportion of the Hartree−Fock (HF) exchange functional (0.428 for MPW1K[6,13,18] and 0.557 for KMLYP,[7] compared to 0.20 for B3-LYP[19]). The optimum balance between the DFT exchange (which is too localized) and the HF exchange (which is too diffuse) is believed to be different for barrier heights,[7,13] compared to stable species (for which the B3-LYP method was originally optimized[19]). The methods also differ from B3-LYP in the specific functionals that they use. The KMLYP method omits the B88 gradient correction term of B3-LYP, for which compensation is made via the inclusion of the larger fraction of HF exchange, and also through a higher-level correction term.[7] The MPW1K method use the modified Perdew-Wang gradient-corrected exchange and the correlation functionals of Adamo and Barone,[20] which are thought to display improved long-range behavior.[6]

These new hybrid DFT techniques have been extensively assessed against (independent) test sets of over 40 hydrogen abstraction reactions that involve the H• radical and were found to display greatly improved performance over B3-LYP. For barrier heights, MPW1K and KMLYP showed mean absolute errors of 7.5 and 3.8 kJ/mol, respectively.[6,7] For reaction enthalpies, the corresponding errors were 7.1 and 5.0 kJ/mol. Thus, these new methods promise excellent low-cost performance for studying hydrogen abstraction reactions in large systems. However, it is important to assess their performance for hydrogen abstraction reactions that involve carbon-centered radicals (which are of interest to the polymer and biochemical fields), particularly when polar effects are important.

In the present work, the accuracy of theoretical procedures for calculating the geometries, barriers, and enthalpies for hydrogen abstraction reactions that involve carbon-centered radicals is assessed, with the aim of identifying reliable yet cost-effective procedures that can be applied to larger systems. To provide a critical test of the alternative computational procedures, the following test set of seven reactions was selected to include the prototypical system (reaction 1), and reactions that involve both strong σ acceptor and donor substituents (reactions 2−4), and strong π acceptor and donor substituents (reactions 5−7).

$$CH_3\bullet + CH_4 \rightarrow CH_4 + CH_3\bullet \qquad (1)$$

$$CH_2F\bullet + CH_4 \rightarrow CH_3F + CH_3\bullet \qquad (2)$$

$$CH_2Li\bullet + CH_4 \rightarrow CH_3Li + CH_3\bullet \qquad (3)$$

$$CH_2Li\bullet + CH_3F \rightarrow CH_3Li + CH_2F\bullet \qquad (4)$$

$$CH_2CN\bullet + CH_4 \rightarrow CH_3CN + CH_3\bullet \qquad (5)$$

$$CH_2OH\bullet + CH_4 \rightarrow CH_3OH + CH_3\bullet \qquad (6)$$

$$CH_2OH\bullet + CH_3CN \rightarrow CH_3OH + CH_2CN\bullet \qquad (7)$$

In the present work, the focus is on the selection of reliable computational procedures for the calculation of accurate electronic-structure information. The reliable calculation of reaction *rates* for hydrogen abstraction reactions is complicated by additional issues, such as the treatment of quantum mechanical tunneling, and will be the subject of a separate study.

2. Theoretical Procedures

Standard ab initio molecular orbital theory[21] and DFT[22] calculations were performed using the GAUSSIAN 98,[23] MOLPRO 2000.6,[24] and ACESII 3.0[25] programs. Unless noted otherwise, calculations on radicals were performed with an unrestricted wave function. In cases where a restricted-open-shell wave function has been used, it is designated with an “R” prefix. The frozen-core approximation was used in all calculations except where full calculations were required as part of a standard composite method.

The objective of this work is to assess the accuracy of various theoretical procedures; therefore, a variety of levels of theory were used for the optimization of geometries and the calculation of barriers and enthalpies. Geometries of the reactants, transition structures, and products in the abstraction reactions 1−7 were optimized using the RHF, HF, RB3-LYP, B3-LYP, MPW1K,[13] KMLYP,[7] RMP2, MP2, QCISD, and (where possible) CCSD(T) methods, in conjunction with a variety of small to large basis sets. Care was taken to ensure that the geometries for each species corresponded to the global (rather than merely local) minimum energy structure by first screening alternative conformations at the HF/6-31G(d) level. To assess the effect of the geometry level on resulting barriers and enthalpies of the reactions, single-point energy calculations were performed on each geometry at the CCSD(T)/6-311+G(d,p) level.

To identify suitable methods for calculating the energies, the barriers and enthalpies for the seven abstraction reactions were then calculated over a wide range of low to very high levels of theory. To assist in the interpretation of the results, the C−H BDEs of the closed-shell CH_3X (X = H, F, Li, CN, OH) molecules and radical stabilization energies (RSEs) of the corresponding $\bullet CH_2X$ radicals (defined as the energy change for the reaction $CH_4 + \bullet CH_2X \rightarrow \bullet CH_3 + CH_3X$) were also calculated. Several high-level composite methods were among the levels of theory considered, including G3X and G3X-(MP2),[26] G3X-RAD and G3X(MP2)-RAD,[2] CBS-QB3,[3,27] and W1.[28,29] For a detailed description of these procedures, the reader is referred to the original references. To explore whether the spin-contamination correction term in the CBS procedures is introducing a systematic error to the calculations of the present work, the energies were also calculated with a modified CBS-QB3 method (denoted as U-CBS-QB3) in which the spin term was omitted. Calculations using several lower-level single-point energies were also included for the purpose of identifying a suitable low-cost procedure for studying larger systems. These included the hybrid DFT methods B3-LYP, RB3-LYP, MPW1K, and KMLYP, and also the RMP2 method, in conjunction with the 6-31+G(d,p) and 6-311+G(3df,2p) basis sets. To ensure that comparisons between the alternative procedures were not obscured by differences in the geometries and zero-point vibrational energy, the energy calculations were performed for geometries at the QCISD/6-311G(d,p) level of theory in all cases, whereas the zero-point vibrational energy was obtained using scaled[30] QCISD/6-31G(d) frequencies. As noted previously, the objective of the present study is to identify reliable theoretical procedures for obtaining the geometries, barriers, and enthalpies in hydrogen abstraction reactions, rather than to predict actual reaction rates or Arrhenius parameters. For this reason, the barriers are reported at 0 K and tunneling corrections are not included.

3. Results and Discussion

3.1. Geometries. Geometries of the reactants, products, and transition structures in reactions 1−7 were optimized at a variety of low to very high levels of theory. The main features of the transition structures for the seven reactions are shown in Figure 1, whereas the corresponding forming- and breaking-bond lengths at a variety of levels of theory are given in Table 1. The geometries of all species (at all levels of theory shown in Table 1) are provided in the Supporting Information.

Examination of Table 1 shows that the transition structure geometries are relatively insensitive to the level of theory. The average deviation from the highest-level values is generally of the order of 0.02 Å, and the maximum deviation is <0.1 Å in all cases. Among the various methods, the QCISD method provides excellent agreement with the considerably more expensive CCSD(T) level of theory, whereas the hybrid DFT methods MPW1K and KMLYP provide excellent low-cost performance. The average deviations from the high-level values are larger with the HF, B3-LYP, and MP2 methods, although, as noted previously, they are still quite small.

To examine the effect of these variations in the geometry level on the calculated barriers and enthalpies, single-point energy calculations were performed on each geometry, using a consistent level of theory (CCSD(T)/6-311+G(d,p)). The resulting barriers and enthalpies are shown in Tables 2 and 3, respectively. Examining the barriers first, we find that the calculated barriers are *generally* insensitive to the level of theory used in the geometry optimization. However, in the case of the reactions that involve the spin-contaminated radical $\bullet CH_2CN$ (e.g., $\langle S^2 \rangle = 0.924$ at the HF/6-31G(d) level of theory), the HF and MP2 methods show errors of 5 kJ/mol, compared to the calculations with the highest-level geometries. The corresponding restricted levels of theory, RHF and RMP2, show slightly improved performance; however, the best low-cost methods are the hybrid DFT procedures, which generally show errors of <1 kJ/mol. Of the alternative procedures, the MPW1K method shows the smallest average deviations, although the B3-LYP and KMLYP procedures also show excellent performance. The QCISD geometries provide an excellent approximation to the more-expensive CCSD(T) geometries and, thus, would be suitable as a benchmark level of theory when the latter cannot be afforded.

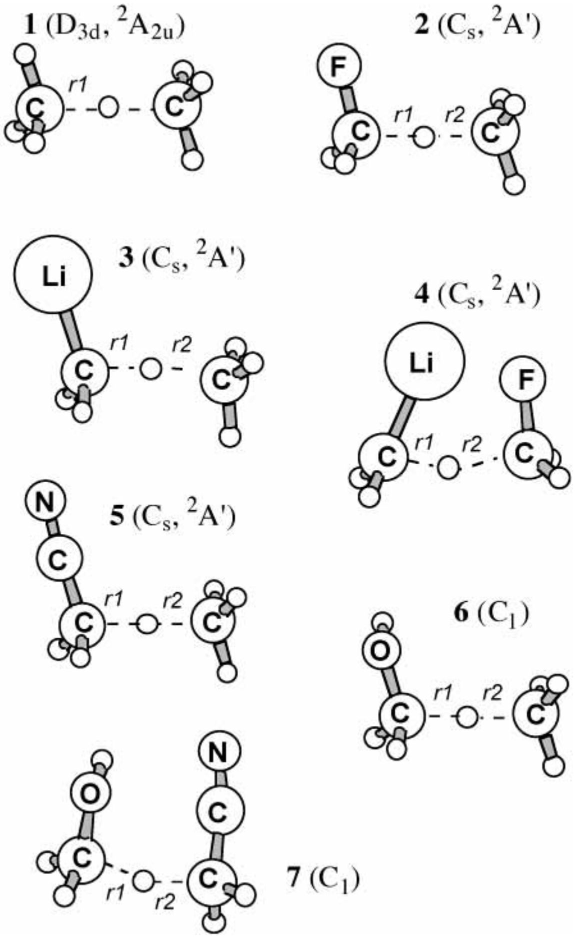

Figure 1. Schematic representation of the transition structures for the hydrogen abstraction reactions. Calculated values for the relevant bond lengths r1 and r2 at a variety of levels of theory are provided in Table 1.

Examining the enthalpies (Table 3) next, we find that the results are similar to those for the barriers. In particular, large errors (up to 7.1 kJ/mol) are observed at the HF and MP2 levels of theory for the reactions that involve the spin-contaminated $\bullet CH_2CN$ radical, and these errors are somewhat reduced, using the corresponding restricted procedures RHF and RMP2. Once again, the QCISD method provides excellent approximations to the high-level geometries, whereas the hybrid DFT procedures provide excellent low-cost performance. Of the alternative DFT procedures, the B3-LYP and MPW1K methods, in conjunction with a small or moderate basis, provide the best performance, showing average deviations of 0.1−0.2 kJ/mol and maximum deviations of up to 0.6 kJ/mol in all cases.

Based on the combined results in Tables 1−3, the main conclusions are that geometry optimizations are relatively insensitive to the level of theory; however, the HF and MP2 methods should be avoided for spin-contaminated systems.

TABLE 1: Effect of Level of Theory on the Forming and Breaking Bond Lengths (Å) in the Optimized Hydrogen Abstraction Transition Structures

level of theory	$H_3C\cdots H\cdots CH_3$	$H_2(F)C\cdots H\cdots CH_3$		$H_2(Li)C\cdots H\cdots CH_3$		$H_2(Li)C\cdots H\cdots CH_2F$		$H_2(CN)C\cdots H\cdots CH_3$		$H_2(OH)C\cdots H\cdots CH_3$		$H_2(OH)C\cdots H\cdots CH_2CN$	
	r1	r1	r2	r1	r2	r1	r2	r1	r2	r1	r2	r1	r2
RHF/6-31G(d)	1.337	1.333	1.337	1.298	1.413	1.270	1.479	1.345	1.329	1.323	1.363	1.315	1.381
HF/6-31G(d)	1.357	1.353	1.359	1.315	1.439	1.285	1.510	1.347	1.369	1.342	1.387	1.351	1.382
HF/6-311G(d,p)	1.357	1.354	1.358	1.315	1.444	1.284	1.512	1.350	1.363	1.340	1.388	1.344	1.388
HF/6-311+G(3df,2pd)	1.356	1.355	1.357	1.315	1.442	1.286	1.507	1.351	1.361	1.342	1.385	1.343	1.388
RB3-LYP/6-31G(d)	1.345	1.319	1.384	1.267	1.466	1.249	1.553	1.303	1.401	1.295	1.433	1.344	1.393
B3-LYP/6-31G(d)	1.348	1.321	1.388	1.269	1.469	1.252	1.552	1.300	1.411	1.296	1.438	1.351	1.388
B3-LYP/6-31G(2df,p)	1.348	1.319	1.392	1.267	1.473	1.249	1.559	1.299	1.411	1.294	1.442	1.349	1.392
B3-LYP/6-311G(d,p)	1.348	1.323	1.381	1.272	1.469	1.257	1.539	1.302	1.406	1.294	1.437	1.345	1.392
B3-LYP/cc-pVTZ	1.347	1.326	1.376	1.275	1.459	1.261	1.525	1.302	1.403	1.298	1.428	1.346	1.386
B3-LYP/6-311+G(3df,2pd)	1.346	1.330	1.371	1.276	1.459	1.261	1.526	1.303	1.401	1.302	1.421	1.346	1.382
MPW1K/6-31G(d)	1.335	1.316	1.362	1.265	1.451	1.227	1.558	1.303	1.374	1.293	1.407	1.325	1.382
MPW1K/6-31+G(d,p)	1.333	1.323	1.349	1.264	1.449	1.219	1.568	1.305	1.367	1.295	1.398	1.319	1.380
MPW1K/6-311+G(3df,2pd)	1.333	1.320	1.353	1.264	1.450	1.230	1.542	1.305	1.366	1.294	1.399	1.318	1.383
KMLYP/6-311+G(3df,2p)	1.326	1.312	1.345	1.258	1.440	1.227	1.520	1.300	1.356	1.286	1.390	1.312	1.382
RMP2/6-31G(d)	1.338	1.276	1.403	1.229	1.494	1.202	1.597	1.276	1.406	1.259	1.442	1.333	1.381
MP2/6-31G(d)	1.332	1.319	1.348	1.269	1.423	1.227	1.538	1.359	1.298	1.299	1.386	1.268	1.441
MP2/6-311G(d,p)	1.327	1.310	1.348	1.258	1.435	1.226	1.526	1.357	1.292	1.286	1.390	1.253	1.457
MP2/6-311+G(3df,2pd)	1.324	1.314	1.339	1.257	1.431	1.220	1.520	1.353	1.290	1.290	1.379	1.254	1.446
QCISD/6-31G(d)	1.347	1.335	1.362	1.286	1.439	1.251	1.545	1.327	1.368	1.316	1.400	1.334	1.391
QCISD/6-311G(d,p)	1.341	1.328	1.359	1.276	1.449	1.243	1.543	1.322	1.362	1.305	1.400	1.323	1.392
CCSD(T)/6-31G(d)	1.347	1.334	1.364	1.283	1.441	1.247	1.554	1.327	1.368				
CCSD(T)/6-311G(d,p)	1.341	1.328	1.357	1.274	1.449	1.242	1.544	1.323	1.356				

TABLE 2: Effect of Geometry on Hydrogen Abstraction Barriers[a]

level of theory for geometry	$CH_3\bullet + CH_4$	$CH_2F\bullet + CH_4$		$CH_2Li\bullet + CH_4$		$CH_2Li\bullet + CH_3F$		$CH_2CN\bullet + CH_4$		$CH_2(OH)\bullet + CH_4$		$CH_2(OH)\bullet + CH_3CN$	
	fwd = rev	fwd	rev	fwd	rev	fwd	rev	fwd	rev	fwd	rev	fwd	rev
RHF/6-31G(d)	78.1	83.8	70.1	91.7	51.4	33.9	7.3	88.8	59.9	94.9	59.9	65.8	59.7
HF/6-31G(d)	78.5	84.5	70.3	92.4	52.2	34.3	8.3	94.7	59.5	95.6	60.3	65.1	64.9
HF/6-311G(d,p)	78.5	84.6	70.4	92.5	52.3	34.3	8.3	95.3	59.4	95.8	60.4	65.5	66.0
HF/6-311+G(3df,2pd)	78.3	84.5	70.3	92.4	52.2	34.3	8.3	95.2	59.1	95.7	60.2	66.1	66.6
RB3-LYP/6-31G(d)	78.2	84.2	70.4	91.9	51.8	35.8	9.5	91.2	60.3	95.7	60.7	65.8	61.7
B3-LYP/6-31G(d)	78.2	84.2	70.4	91.9	51.8	35.7	9.4	90.8	60.1	95.8	60.7	65.8	61.5
B3-LYP/6-31G(2df,p)	78.2	84.1	70.4	91.8	51.8	35.4	9.1	90.7	60.0	95.7	60.7	65.9	61.6
B3-LYP/6-311G(d,p)	78.2	83.9	70.5	92.0	51.9	35.2	8.6	91.0	60.0	95.7	60.8	65.6	61.7
B3-LYP/cc-pVTZ	78.2	83.9	70.6	92.1	51.9	34.8	7.9	91.1	60.1	95.6	61.0	65.6	61.9
B3-LYP/6-311+G(3df,2pd)	78.2	83.9	70.7	92.1	52.0	34.9	7.9	91.2	60.1	95.6	61.1	65.8	62.4
MPW1K/6-31G(d)	78.0	84.4	70.5	91.9	51.8	34.7	8.6	91.6	60.1	95.9	60.7	65.6	61.8
MPW1K/6-31+G(d,p)	78.2	84.2	70.7	92.1	51.9	34.9	8.2	91.7	60.2	95.8	61.0	65.6	62.2
MPW1K/6-311+G(3df,2pd)	78.1	83.9	70.8	92.1	51.9	35.1	8.1	91.9	60.1	95.5	61.1	65.0	62.3
KMLYP/6-311+G(3df,2p)	78.2	83.9	71.1	92.1	52.1	36.1	8.9	92.2	60.2	95.3	61.2	65.4	63.3
RMP2/6-31G(d)	78.0	82.4	68.8	91.3	50.9	34.9	8.0	90.1	59.4	94.3	59.4	67.5	63.3
MP2/6-31G(d)	78.2	84.4	70.9	92.3	51.9	35.0	8.1	87.8	60.4	95.8	60.9	65.8	58.2
MP2/6-311G(d,p)	78.3	84.5	70.8	92.2	52.0	35.1	8.6	86.9	62.1	96.0	61.0	67.1	56.9
MP2/6-311+G(3df,2pd)	78.3	84.4	70.9	92.3	52.1	34.9	8.2	86.6	62.7	95.9	61.1	68.0	57.1
QCISD/6-31G(d)	78.2	84.3	70.8	92.1	51.8	34.9	8.0	91.6	60.6	95.8	60.9	65.4	61.5
QCISD/6-311G(d,p)	78.1	84.3	70.6	92.0	51.8	34.8	8.2	91.5	60.4	95.9	60.8	65.4	61.5
CCSD(T)/6-31G(d)	78.2	84.3	70.8	92.2	51.8	35.0	8.1	91.6	60.6				
CCSD(T)/6-311G(d,p)	78.1	84.3	70.7	92.0	51.8	35.0	8.4	91.8	60.7				

[a] Calculated at the CCSD(T)/6-311+G(d,p) level of theory. Values given in units of kJ/mol. 0 K values and zero-point vibrational energy not included.

Problems with these latter methods have previously been reported for other types of radical reactions, such as radical addition to alkenes,[31,32] and may well be a general feature of radical reactions. The hybrid DFT methods provide excellent low-cost performance, with a method such as MPW1K/6-31+G(d,p) being preferred for reaction barriers. The QCISD method provides an excellent benchmark level of theory for optimizing the geometries for these reactions.

3.2. Thermochemistry. Having studied the effects of geometry, the enthalpies for the seven reactions were calculated at a variety of levels of theory, using a consistent set of geometries (optimized at the QCISD/6-311G(d,p) level of theory), and the results are shown in Table 4. The highest-level procedure included in the study is the W1 method, which approximates coupled cluster energies [URCCSD(T)] with an infinite basis set using extrapolation procedures, and includes corrections for core correlation, relativistic effects, and spin−orbit coupling in atoms. As noted previously, when assessed against large test sets of experimental thermochemical data, this method has been observed to display deviations from experiment of <2 kJ/mol.[4] The W1 method is thus treated as the benchmark level of theory in the current study, and the mean absolute deviation (MAD) from the corresponding W1 results at the other levels of theory is included in Table 4. Where available, corresponding gas-phase experimental values are also included in Table 4. These were calculated using the experimental values for the BDEs of the closed-shell CH_3X species at 0 K, as reported in ref 8.

Comparing the alternative composite procedures first, we find that there is generally excellent agreement among the alternative methods. The largest MAD occurs for the CBS-QB3 procedure (2.2 kJ/mol); in all other cases, the MADs are 1.1 kJ/mol or less. On closer examination, we find that the CBS-QB3

TABLE 3: Effect of Geometry on Hydrogen Abstraction Enthalpies[a]

level of theory for geometry	$CH_3\bullet + CH_4$	$CH_2F\bullet + CH_4$	$CH_2Li\bullet + CH_4$	$CH_2Li\bullet + CH_3F$	$CH_2CN\bullet + CH_4$	$CH_2(OH)\bullet + CH_4$	$CH_2(OH)\bullet + CH_3CN$
RHF/6-31G(d)	0.0	13.7	40.3	26.6	28.9	35.0	6.0
HF/6-31G(d)	0.0	14.1	40.2	26.0	35.1	35.3	0.2
HF/6-311G(d,p)	0.0	14.2	40.1	25.9	36.0	35.4	−0.6
HF/6-311+G(3df,2pd)	0.0	14.2	40.2	26.0	36.1	35.6	−0.5
RB3-LYP/6-31G(d)	0.0	13.8	40.1	26.3	30.9	35.0	4.1
B3-LYP/6-31G(d)	0.0	13.8	40.1	26.3	30.7	35.1	4.3
B3-LYP/6-31G(2df,p)	0.0	13.8	40.1	26.3	30.7	35.0	4.3
B3-LYP/6-311G(d,p)	0.0	13.4	40.0	26.6	31.0	34.9	3.8
B3-LYP/cc-pVTZ	0.0	13.3	40.2	26.9	31.1	34.7	3.6
B3-LYP/6-311+G(3df,2pd)	0.0	13.2	40.1	27.0	31.0	34.4	3.4
MPW1K/6-31G(d)	0.0	14.0	40.1	26.2	31.4	35.2	3.7
MPW1K/6-31+G(d,p)	0.0	13.5	40.2	26.6	31.5	34.9	3.4
MPW1K/6-311+G(3df,2pd)	0.0	13.1	40.2	27.0	31.8	34.5	2.6
KMLYP/6-311+G(3df,2p)	0.0	12.8	40.0	27.2	32.0	34.1	2.1
RMP2/6-31G(d)	0.0	13.5	40.4	26.9	30.8	35.0	4.2
MP2/6-31G(d)	0.0	13.5	40.4	26.9	27.4	34.9	7.5
MP2/6-311G(d,p)	0.0	13.6	40.2	26.6	24.8	35.0	10.2
MP2/6-311+G(3df,2pd)	0.0	13.5	40.3	26.7	23.9	34.8	10.9
QCISD/6-31G(d)	0.0	13.5	40.3	26.8	30.9	34.8	3.9
QCISD/6-311G(d,p)	0.0	13.7	40.2	26.5	31.2	35.0	3.9
CCSD(T)/6-31G(d)	0.0	13.5	40.4	26.9	31.0	34.9	3.9
CCSD(T)/6-311G(d,p)	0.0	13.6	40.2	26.6	31.0	35.0	4.0

[a] Calculated at the CCSD(T)/6-311+G(d,p) level of theory. Values given in units of kJ/mol. 0 K values and zero-point vibrational energy not included.

TABLE 4: Effect of Level of Theory on Hydrogen Abstraction Enthalpies[a]

level of theory	$CH_3\bullet + CH_4$	$CH_2F\bullet + CH_4$	$CH_2Li\bullet + CH_4$	$CH_2Li\bullet + CH_3F$	$CH_2CN\bullet + CH_4$	$CH_2(OH)\bullet + CH_4$	$CH_2(OH)\bullet + CH_3CN$	MAD[b]
MPW1K/6-31+G(d,p)	0	13.4	31.6	18.2	38.0	33.9	−4.1	2.4
MPW1K/6-311+G(3df,2p)	0	14.9	34.2	19.3	37.3	34.8	−2.5	2.2
KMLYP/6-31+G(d,p)	0	13.9	33.0	19.1	38.6	35.5	−3.2	2.4
KMLYP/6-311+G(3df,2p)	0	15.2	35.2	20.0	37.8	36.8	−0.9	2.5
B3LYP/6-31+G(d,p)	0	15.7	34.1	18.4	44.3	38.0	−6.4	4.8
B3LYP/6-311+G(3df,2p)	0	17.5	35.6	18.1	43.9	39.1	−4.8	5.3
RB3LYP/6-31+G(d,p)	0	15.9	34.9	19.0	40.3	38.2	−2.1	3.5
RB3LYP/6-311+G(3df,2p)	0	17.6	36.4	18.8	40.0	39.3	−0.7	4.0
RMP2/6-31+G(d,p)	0	8.3	29.0	20.6	29.9	29.0	−0.9	3.1
RMP2/6-311+G(3df,2p)	0	12.3	30.9	18.6	31.0	32.1	1.0	1.3
G3X(MP2)	0	13.0	32.3	19.3	32.6	32.8	0.3	0.6
G3X	0	12.4	33.4	21.0	33.1	32.7	−0.5	0.7
G3X(MP2)-RAD	0	11.8	31.7	20.0	31.9	31.6	−0.2	1.1
G3X-RAD	0	12.4	33.3	20.8	33.0	32.7	−0.2	0.6
CBS-QB3	0	13.3	34.1	20.8	38.3	33.8	−4.5	2.2
U−CBS-QB3	0	13.4	34.2	20.8	33.5	33.8	0.3	0.6
W1	0	13.0	33.1	20.2	32.7	33.6	1.0	0
experiment[c]	0	14.8 ± 5			41.7 ± 4.8	35.9 ± 1.7	−5.8 ± 6.5	

[a] At 0 K. Values are given in units of kJ/mol. Based on QCISD/6-311G(d,p) geometries and includes zero-point vibrational energy at the QCISD/6-31G(d) level of theory. [b] Mean absolute deviation. [c] Calculated using the experimental values for the bond dissociation energies of the CH_3X species reported in ref 8 and references therein.

procedure also shows deviations from W1 of 1 kJ/mol or less, except for the two reactions that involve the spin-contaminated $\bullet CH_2CN$ radical, for which larger deviations (5.5−5.6 kJ/mol) occur. In these cases, the deviations from W1 (and the other composite methods) are reduced considerably when the correction term in the CBS method is omitted (i.e., the U-CBS-QB3 procedure). This mirrors the earlier results for radical addition barriers[9,10] and N−H BDEs[11] and suggests that the (empirically based) spin-contamination correction term in the CBS procedures may be overestimating the effects of spin contamination in these radical reactions. Indeed, an alternative estimate of the errors due to spin contamination may be obtained by comparing corresponding "RAD" and "non-RAD" versions of the G3 methods, for which the principal difference is the use of restricted-open shell and unrestricted procedures, respectively. For the two spin-contaminated systems of the present work, the difference between the enthalpies obtained with corresponding RAD and non-RAD G3 procedures is <1 kJ/mol, and this is considerably less than the spin-correction term in the CBS-QB3 procedure for these reactions (4.8 kJ/mol).

The comparisons against the benchmark W1 values (and the other composite procedures) thus suggest that the spin-correction term is introducing a systematic error to the CBS-QB3 enthalpies for the spin-contaminated reactions. However, in contrast to this result, when the calculated reaction enthalpies are compared with the available gas-phase experimental values, we find that the spin-corrected CBS-QB3 procedure actually shows the closest agreement with the experimental values. Hence, it would seem that either the spin-correction term in the CBS methods is correct (and there is, thus, a problem with URCCSD(T) theory in spin-contaminated systems) or, alternatively, the experimental values may be in error. To probe this question further, the corresponding C−H BDEs for the closed-shell CH_3X species and RSEs for the open-shell $\bullet CH_2X$ species were calculated at the various levels of theory, and the results are shown in Table 5. The performance of various levels of theory for predicting these quantities have been assessed previously;[8] however, the values are of interest in the present work because the enthalpies for the hydrogen abstraction reactions can be calculated as the difference of the BDEs of the respective closed-shell species

TABLE 5: Effect of Level of Theory on Radical Stabilization Energies (RSEs) of the Alkyl Radicals (R•) and Corresponding R−H Bond Dissociation Energies (BDEs) of the Closed-Shell Species[a]

	•CH_3		•CH_2F		•CH_2Li		•CH_2CN		•CH_2OH		MAD[b]	
level of theory	BDE	RSE	BDE	RSE	BDE	RSE	BDE	RSE	BDE	RSE	BDEs	RSEs
MPW1K/6-31+G(d,p)	419.1	0	405.7	13.4	387.4	31.6	381.1	38.0	385.2	33.9	12.6	1.9
MPW1K/6-311+G(3df,2p)	414.7	0	399.8	14.9	380.5	34.2	377.4	37.3	379.9	34.8	17.8	2.2
KMLYP/6-31+G(d,p)	448.1	0	434.2	13.9	415.1	33.0	409.5	38.6	412.7	35.5	15.6	2.2
KMLYP/6-311+G(3df,2p)	444.1	0	428.9	15.2	408.9	35.2	406.3	37.8	407.2	36.8	10.8	3.2
B3LYP/6-31+G(d,p)	428.7	0	413.0	15.7	394.6	34.1	384.3	44.3	390.7	38.0	6.0	4.9
B3LYP/6-311+G(3df,2p)	424.2	0	406.7	17.5	388.5	35.6	380.3	43.9	385.1	39.1	11.3	5.9
RB3LYP/6-31+G(d,p)	432.3	0	416.4	15.9	397.4	34.9	392.0	40.3	394.1	38.2	2.5	4.2
RB3LYP/6-311+G(3df,2p)	428.4	0	410.7	17.6	392.0	36.4	388.4	40.0	389.1	39.3	6.6	5.2
RMP2/6-31+G(d,p)	409.8	0	401.5	8.3	380.9	29.0	379.9	29.9	380.8	29.0	17.7	4.1
RMP2/6-311+G(3df,2p)	416.9	0	404.6	12.3	386.1	30.9	385.9	31.0	384.8	32.1	12.6	1.5
G3X(MP2)	428.1	0	415.1	13.0	395.8	32.3	395.5	32.6	395.2	32.8	2.4	0.4
G3X	429.0	0	416.6	12.4	395.6	33.4	395.8	33.1	396.3	32.7	1.6	0.5
G3X(MP2)-RAD	428.0	0	416.3	11.8	396.3	31.7	396.2	31.9	396.4	31.6	1.7	1.4
G3X-RAD	430.2	0	417.8	12.4	396.9	33.3	397.2	33.0	397.5	32.7	0.5	0.5
CBS-QB3	433.1	0	419.8	13.3	398.9	34.1	394.8	38.3	399.2	33.8	2.2	1.8
U−CBS-QB3	433.4	0	420.0	13.4	399.2	34.2	399.8	33.5	399.5	33.8	2.1	0.6
W1	430.8	0	417.8	13.0	397.6	33.1	398.1	32.7	397.2	33.6	0	0
experiment[c]	432.2 ± 0.4	0	417.4 ± 4	14.8 ± 5			390.5 ± 4.4	41.7 ± 4.8	396.3 ± 1.3	35.9 ± 1.7		

[a] At 0 K. Values are given in units of kJ/mol. Based on QCISD/6-311G(d,p) geometries and includes zero-point vibrational energy at the QCISD/6-31G(d) level of theory. [b] Mean absolute deviation from the corresponding W1 value. [c] As reported in ref 8.

in the reaction, or alternatively, the difference of the RSEs of the corresponding open-shell species.

Through examination of Table 4, we note that, as in the case of the enthalpies, there is generally good agreement among the various methods, except in the case of the spin-contaminated •CH_2CN radical. In this case, the non-spin-corrected CBS method is in accord with the other composite methods, but the spin-corrected CBS method is closer to (but still differs from) the experimental value. Thus, the deviation from experiment in the spin-contaminated reactions arises from a single experimental value (the C−H BDE of CH_3CN), and even the spin-corrected CBS procedure shows some deviation from the measured result in this case. In all other cases, the BDEs and RSEs are in good agreement with the experimental values, with the W1 method showing deviations of 1.4 kJ/mol or less for BDEs and 2.3 kJ/mol for RSEs (which are, effectively, differences of BDEs). Therefore, it is possible that the experimental value for the CH_3CN case may require some adjustment, and a re-examination of this system would be helpful. In the meantime, the balance of evidence—both from the abstraction reactions of the present work, and also earlier studies of radical addition barriers[9,10] and N−H BDEs[11]—suggests that the spin-correction term in the CBS-type procedures may be overestimating the effects of spin contamination in these reactions, and the G3-RAD-type procedures (which avoid the need for this term through the use of restricted-open shell methods) should be preferred when the high-level W1 method cannot be afforded.

It is also important to identify accurate lower-cost procedures, which can be used on larger polymer-related or biochemical-related systems, when composite procedures cannot be afforded. To this end, the enthalpies calculated using lower levels of theory, such as various hybrid DFT methods and the RMP2 method, are included in Table 5. Examination of these results shows that the most-expensive low-level method, RMP2/6-311+G(3df,2p), provides the closest approximations to W1, showing an MAD of just 1.3 kJ/mol and a maximum deviation of just 2.2 kJ/mol. The good performance of RMP2 has also been reported for other radical reactions, including radical addition to alkenes,[10,31] to carbonyls,[17] and to thiocarbonyl compounds,[9] although not radical addition to alkynes.[10] Of the lower-cost methods, the new hybrid DFT procedures, MPW1K and KMLYP, also show excellent agreement with the considerably more-expensive W1 values. Even in conjunction with a small basis set such as 6-31+G(d,p), both procedures have MADs of only 2.4 kJ/mol for the seven reactions, and maximum deviations of up to 5.9 kJ/mol (for the spin-contaminated reactions) and up to 2 kJ/mol (for the other cases). The performance of these new hybrid DFT methods is superior to that of the B3-LYP method, for which MADs of up to 5.3 kJ/mol and maximum deviations of up to 11.6 kJ/mol are observed, and this is in accord with the conclusions from studies of other types of hydrogen abstraction reactions.[6,7] It can also be observed that the RB3-LYP method shows improved performance over (U) B3-LYP, although the MPW1K and KMLYP results are superior to both B3-LYP procedures.

Interestingly, when we examine the BDEs (see Table 5), we find that the B3-LYP methods show the closest agreement with the high-level W1 values. For example, for the 6-31+G(d,p) basis set, the MADs for the various procedures are 12.6 kJ/mol (MPW1K), 15.6 kJ/mol (KMLYP), 6.0 kJ/mol (B3-LYP), 2.5 kJ/mol (RB3-LYP), and 17.7 kJ/mol (RMP2). The superior performance of the MPW1K, KMLYP, and RMP2 methods for enthalpies and RSEs (which are differences of BDEs) thus occurs through substantial cancellation of error. These methods seem to provide more-accurate *relative* values for BDEs, compared to B3-LYP, but less-accurate *absolute* values. This failure of B3-LYP to produce accurate relative BDEs has also been noted recently for the case of R−X BDEs (where R = Me, Et, *i*-Pr, and *t*-Bu, and X = H, CH_3, OCH_3, OCH_2, OH, and F), where the B3-LYP method even failed to reproduce the correct qualitative ordering for the alkyl substituent effects on the R−X BDEs when X was an electronegative substituent, such as OH or OCH_3.[17] As in the present work, the RMP2/6-311+G(3df,2p) method provided good agreement with experiment and also with higher-level values for the relative BDEs, but somewhat poorer agreement for the absolute BDEs. The good performance of the RMP2 method for predicting RSEs (which are also differences of BDEs) over a large test set of CH_3X species was also noted in ref 8. Hence, although the good performance of MPW1K, KMLYP, and RMP2 for predicting reaction enthalpies results in the systematic cancellation of errors in the relative BDEs of the alternate closed-shell molecules, there is some evidence (at least for RMP2) that this might be

TABLE 6: Effect of Level of Theory on Hydrogen Abstraction Barriers[a]

level of theory	$CH_3\bullet + CH_4$	$CH_2F\bullet + CH_4$		$CH_2Li\bullet + CH_4$		$CH_2Li\bullet + CH_3F$		$CH_2CN\bullet + CH_4$		$CH_2(OH)\bullet + CH_4$		$CH_2(OH)\bullet + CH_3CN$		MAD[b]
	fwd = rev	fwd	rev	fwd	rev	fwd	rev	fwd	rev	fwd	rev	fwd	rev	
MPW1K/6-31+G(d,p)	68.6	73.0	59.6	77.9	46.3	22.3	4.1	86.9	48.9	83.9	50.1	54.0	58.1	3.6
MPW1K/6-311+G(3df,2p)	70.5	75.3	60.4	81.6	47.4	27.1	7.8	87.9	50.6	86.8	51.9	57.4	59.9	2.4
KMLYP/6-31+G(d,p)	61.3	66.2	52.3	72.3	39.4	12.1	−7.0	80.6	42.0	78.4	43.0	45.8	49.0	11.0
KMLYP/6-311+G(3df,2p)	63.6	69.7	54.6	76.4	41.2	16.8	−3.2	82.0	44.2	83.3	46.5	48.4	49.4	7.9
B3LYP/6-31+G(d,p)	61.5	66.7	51.0	72.2	38.1	12.3	−6.1	84.3	40.0	78.9	40.9	47.1	53.4	11.1
B3LYP/6-311+G(3df,2p)	64.6	70.1	52.6	75.8	40.2	15.2	−3.0	86.5	42.7	83.1	44.0	50.5	55.3	8.2
RB3LYP/6-31+G(d,p)	63.7	69.0	53.1	74.5	39.6	15.1	−3.9	82.4	42.1	81.0	42.8	48.8	50.9	9.3
RB3LYP/6-311+G(3df,2p)	66.3	72.2	54.5	77.7	41.3	17.5	−1.3	84.7	44.7	84.9	45.6	52.1	52.7	6.7
RMP2/6-31+G(d,p)	76.3	77.6	69.3	81.8	52.9	28.9	8.3	86.8	56.9	89.0	60.0	54.2	55.2	2.6
RMP2/6-311+G(3df,2p)	68.0	72.8	60.5	74.5	43.6	26.2	7.6	80.0	48.9	84.1	52.0	46.6	45.6	4.5
G3X(MP2)	76.8	81.3	68.4	82.5	50.2	27.0	7.6	88.3	55.8	91.5	58.6	58.4	58.1	2.4
G3X	76.9	80.4	68.0	83.6	50.2	26.0	4.9	89.1	56.0	91.0	58.3	57.8	58.3	2.1
G3X(MP2)-RAD	75.1	79.2	67.4	80.4	48.7	26.1	6.1	88.4	56.6	89.1	57.4	57.6	57.8	1.2
G3X-RAD	74.8	78.9	66.5	81.9	48.6	26.0	5.2	88.4	55.4	89.3	56.6	57.1	57.3	0.9
CBS-QB3	71.8	75.8	62.5	79.0	44.9	25.3	4.5	87.8	49.5	86.5	52.7	51.2	55.7	2.1
U−CBS-QB3	72.5	76.5	63.2	79.8	45.6	26.1	5.3	85.3	51.8	87.2	53.4	53.8	53.5	1.5
W1	73.3	78.1	65.1	80.7	47.5	25.4	5.3	87.1	54.4	89.2	55.5	−	−	0

[a] At 0 K. Values are given in units of kJ/mol. Based on QCISD/6-311G(d,p) geometries and includes zero-point vibrational energy at the QCISD/6-31G(d) level of theory. Throughout the table, fwd = forward reaction and rev = reverse reaction. [b] Mean absolute deviation from the corresponding W1 value.

expected to be general for hydrogen abstraction reactions that involve transfer between carbon-centered radicals.

3.3. Barriers. Barriers for the seven hydrogen abstraction reactions were also calculated at a variety of levels of theory, using the consistent set of QCISD/6-311G(d,p) geometries, and the results are shown in Table 6. As in the case of the enthalpies, the results at the various levels of theory were benchmarked against the highest-level W1 values, and the MADs at each level of theory are included in Table 6.

Comparisons with experiment have not been performed for the reaction barriers in the present work, because several additional issues complicate such comparisons. Even for gas-phase experimental values, the measured reaction rates k at a specific temperature T must be related to the calculated reaction barriers at 0 K (E_0) via an assumed model, such as transition-state theory (eq 8):

$$k(T) = \kappa\left(\frac{k_B T}{h}\right)\left(\frac{Q_\ddagger}{\prod\limits_{\text{reactants}} Q_i}\right)\exp\left(-\frac{E_0}{RT}\right) \tag{8}$$

where κ is the tunneling coefficient, $Q_\ddagger$ the molecular partition function of the transition structure (and Q_i the molecular partition function of reactant i), k_B the Boltzmann constant, h Planck's constant, and R the universal gas constant. To obtain an "experimental" value of E_0 from a measured reaction rate, values for the partition functions and the tunneling coefficient are required, and these may be obtained via ab initio calculations. In performing these additional calculations, a specific level of theory must be chosen, and further assumptions (such as the method for treating low-frequency torsional modes and for calculating the tunneling coefficient) must be made. The accuracy of the calculated partition functions and tunneling coefficients are very sensitive to both the methods used to calculate them and the level of theory at which they are applied, and errors in these values may obscure quantitative comparisons between the theoretical and experimental barriers. To facilitate a rigorous comparison with experimental values, an assessment of the accuracy of the calculated rate and tunneling coefficients (obtained via various methods and at various levels of theory) will be the subject of a separate study. In the present work, the barriers are compared internally against the W1 values, which, as noted previously, is a very high level of theory that has been previously demonstrated to provide accurate thermochemical data.[4]

Examining the high-level barriers in Table 6 first, we find that there is again excellent agreement among the alternative composite methods, with all methods having MADs of 2.4 kJ/mol or less and maximum deviations of <5 kJ/mol, when compared with W1. The RAD versions of G3 perform slightly better than the corresponding non-RAD G3 methods and, thus, would be preferred as a benchmark level of theory when W1 cannot be afforded. As in the case of the enthalpies, the non-spin-corrected CBS method performs better than the spin-corrected method, particularly in the reactions that produce the spin-contaminated $\bullet CH_2CN$ radical. This again suggests that the spin-correction term may be introducing a systematic error to the CBS values. The development of a restricted open-shell version of the CBS procedure, or a refinement of the spin-correction term, would thus be advisable.

Examining the lower-level values next, we find that the MPW1K method again performs very well when compared with the highest-level values. With the large 6-311+G(3df,2p) basis set, the MAD is just 2.4 kJ/mol, and the maximum deviation is 4.7 kJ/mol. The performance of the KMLYP level of theory is somewhat poorer for reaction barriers (MAD = 7.9 kJ/mol, maximum deviation of 10.5 kJ/mol) and is only slightly better than B3-LYP (MAD = 8.2 kJ/mol, maximum deviation of 12.5 kJ/mol) and is actually slightly poorer than RB3-LYP (MAD = 6.7 kJ/mol, maximum deviation of 10.6 kJ/mol). The RMP2 method again shows good agreement with the highest-level values, although interestingly, the smaller basis set values (MAD = 2.6 kJ/mol, maximum deviation of 5.4 kJ/mol) are more similar to the W1 values than the larger basis set values (MAD = 4.5 kJ/mol, maximum deviation of 7.1 kJ/mol). Based on the combined performance of the alternative lower-level procedures for calculating the barriers and enthalpies of the hydrogen abstraction reactions, the MPW1K method, in conjunction with a large basis set such as 6-311+G(3df,2p), should provide an excellent low-cost procedure for studying H-atom abstraction reactions between carbon-centered radicals, which reinforces the earlier conclusions derived from studies of other types of H-atom abstraction reactions.[6]

4. Conclusions

On the basis of the aforementioned assessment of procedures for calculating the geometries, barriers, and enthalpies in hydrogen abstraction reactions that involve carbon-centered radicals, the following conclusions may be drawn:

(1) Calculated geometries are relatively insensitive to the level of theory; however, the Hartree–Fock (HF) and Möller–Plesset second-order perturbation (MP2) methods should be avoided for spin-contaminated systems. Problems with these latter methods have previously been reported for other types of radical reactions, such as radical addition to alkenes,[31,32] and may well be a general feature of radical reactions. The QCISD/6-31G(d) method provides an excellent benchmark level of theory for optimizing the geometries for these reactions, when higher-level calculations cannot be afforded. For larger systems, the hybrid DFT methods provide excellent low-cost performance, with a method such as MPW1K/6-31+G(d,p) providing the best overall performance.

(2) The calculated barriers and enthalpies are more sensitive to the level of theory. Nonetheless, the various types of composite methods show good agreement with each other, except in the case of spin-contaminated reactions. In those cases, the spin-correction term in the CBS procedures seems to be introducing a systematic error to the calculated values. This mirrors earlier results for radical addition barriers[9,10] and N–H bond dissociation energies (BDEs)[11] and suggests that this term may require some adjustment. Overall, the "RAD" variants of G3 show slightly better agreement with the highest-level W1 values than the corresponding "non-RAD" G3 methods, and would hence be preferred as a benchmark level of theory when W1 cannot be afforded.

(3) For larger systems, a variety of low-level methods were examined. For reaction enthalpies, the RMP2, MPW1K, and KMLYP procedures showed excellent agreement with the higher-level values, whereas for barriers, the best performance was obtained with the MPW1K and RMP2 methods. The best overall performance was provided by the MPW1K/6-311+G(3df,2p) method, although the RMP2/6-311+G(3df,2p) might be preferred if accurate thermochemistry were the main focus.

Acknowledgment. Generous allocations of computing time on the Compaq Alphaserver of the National Facility of the Australian Partnership for Advanced Computing and the Australian National University Supercomputing Facility, useful discussions with Professor Leo Radom, assistance with the KMLYP calculations from Professor Charles Musgrave, and the provision of an Australian Research Council postdoctoral fellowship to the author are all gratefully acknowledged.

Supporting Information Available: Table S1, showing all optimized geometries in the form of GAUSSIAN archive entries (PDF). This material is available free of charge via the Internet at http://pubs.acs.org.

References and Notes

(1) Curtiss, L. A.; Raghavachari, K. *Theor. Chem. Acc.* **2002**, *108*, 61–70.

(2) Henry, D. J.; Sullivan, M. B.; Radom, L. *J. Chem. Phys.* **2003**, *118*, 4849–4860.

(3) Montgomery, J. A., Jr.; Frisch, M. J.; Ochterski, J. W.; Petersson, G. A. *J. Chem. Phys.* **2000**, *112*, 6532–6542.

(4) Martin, J. M. L.; Parthiban, S. In *Quantum Mechanical Prediction of Thermochemical Data*; Cioslowski, J., Ed.; Kluwer-Academic: Dordrecht, The Netherlands, 2001; pp 31–65.

(5) Raghavachari, K.; Curtiss, L. A. In *Quantum Mechanical Prediction of Thermochemical Data*; Cioslowski, J., Ed.; Kluwer-Academic: Dordrecht, The Netherlands, 2001; pp 67–98.

(6) Lynch, B. J.; Truhlar, D. G. *J. Phys. Chem. A* **2001**, *105*, 2936–2941.

(7) Kang, J. K.; Musgrave, C. B. *J. Chem. Phys.* **2001**, *115*, 11040.

(8) Henry, D. J.; Parkinson, C. J.; Mayer, P. M.; Radom, L. *J. Phys. Chem. A* **2001**, *105*, 6750–6756.

(9) Coote, M. L.; Wood, G. P. F.; Radom, L. *J. Phys. Chem. A* **2002**, *106*, 12124–12138.

(10) Gómez-Balderas, R.; Coote, M. L.; Henry, D. J.; Radom, L. Reliable Theoretical Procedures for Calculating the Rate of Methyl Radical Addition to Carbon–Carbon Double and Triple Bonds. *J. Phys. Chem. A* **2004**, in press.

(11) Wood, G. P. F.; Henry, D. J.; Radom, L. *J. Phys. Chem. A* **2003**, *107*, 7985–7990.

(12) Kohn, W.; Becke, A. D.; Parr, R. G. *J. Phys. Chem.* **1996**, *100*, 12974–12980.

(13) Lynch, B. J.; Fast, P. L.; Harris, M.; Truhlar, D. G. *J. Phys. Chem. A* **2000**, *104*, 4811–4815.

(14) Basch, H.; Hoz, S. *J. Phys. Chem. A* **1997**, *101*, 4416.

(15) Jursic, B. S. *Chem. Phys. Lett.* **1997**, *264*, 113.

(16) Saeys, M.; Reyniers, M.-F.; Marin, G. B.; van Speybroeck, V.; Waroquier, M. *J. Phys. Chem. A* **2003**, *107*, 9147–9159.

(17) Coote, M. L.; Pross, A.; Radom, L. In *Fundamental World of Quantum Chemistry: A Tribute to the Memory of Per-Olov Löwdin*, Vol. III. Brändas, E. J., Kryachko, E. J., Eds.; Kluwer-Springer: New York, 2004 (in press).

(18) Lynch, B. J.; Truhlar, D. G. *J. Phys. Chem. A* **2002**, *106*, 842–846.

(19) Becke, A. D. *J. Chem. Phys.* **1993**, *98*, 5648.

(20) Adamo, C.; Barone, V. *J. Chem. Phys.* **1998**, *108*, 664.

(21) Hehre, W. J.; Radom, L.; Schleyer, P. v. R.; Pople, J. A. *Ab Initio Molecular Orbital Theory*; Wiley: New York, 1986.

(22) Koch, W.; Holthausen, M. C. *A Chemist's Guide to Density Functional Theory*; Wiley-VCH: Weinheim, Germany, 2000.

(23) Frisch, M. J.; Trucks, G. W.; Schlegel, H. B.; Scuseria, G. E.; Robb, M. A.; Cheeseman, J. R.; Zakrzewski, V. G.; Montgomery, J. A., Jr.; Stratmann, R. E.; Burant, J. C.; Dapprich, S.; Millam, J. M.; Daniels, A. D.; Kudin, K. N.; Strain, M. C.; Farkas, O.; Tomasi, J.; Barone, V.; Cossi, M.; Cammi, R.; Mennucci, B.; Pomelli, C.; Adamo, C.; Clifford, S.; Ochterski, J.; Petersson, G. A.; Ayala, P. Y.; Cui, Q.; Morokuma, K.; Malick, D. K.; Rabuck, A. D.; Raghavachari, K.; Foresman, J. B.; Cioslowski, J.; Ortiz, J. V.; Stefanov, B. B.; Liu, G.; Liashenko, A.; Piskorz, P.; Komaromi, I.; Gomperts, R.; Martin, R. L.; Fox, D. J.; Keith, T.; Al-Laham, M. A.; Peng, C. Y.; Nanayakkara, A.; Gonzalez, C.; Challacombe, M.; Gill, P. M. W.; Johnson, B. G.; Chen, W.; Wong, M. W.; Andres, J. L.; Head-Gordon, M.; Replogle, E. S.; Pople, J. A. *Gaussian 98*, revision A.11, Gaussian, Inc.: Pittsburgh, PA, 1998.

(24) Werner, H.-J.; Knowles, P. J.; Amos, R. D.; Bernhardsson, A.; Berning, A.; Celani, P.; Cooper, D. L.; Deegan, M. J. O.; Dobbyn, A. J.; Eckert, F.; Hampel, C.; Hetzer, G.; Korona, T.; Lindh, R.; Lloyd, A. W.; McNicholas, S. J.; Manby, F. R.; Meyer, W.; Mura, M. E.; Nicklass, A.; Palmieri, P.; Pitzer, R.; Rauhut, G.; Schütz, M.; Stoll, H.; Stone, A. J.; Tarroni, R.; Thorsteinsson, T. *MOLPRO 2000.6*; University of Birmingham: Birmingham, U.K., 1999.

(25) Stanton, J. F.; Gauss, J.; Watts, J. D.; Nooijen, M.; Oliphant, N.; Perera, S. A.; Szalay, P. G.; Lauderdale, W. J.; Kucharski, S. A.; Gwaltney, S. R.; Beck, S.; Balková, A.; Bernholdt, D. E.; Baeck, K. K.; Rozyczko, P.; Sekino, H.; Hober, C.; Bartlett, R. J. *ACES II: Quantum Theory Project*; University of Florida: Gainsville, FL, 1992.

(26) Curtiss, L. A.; Redfern, P. C.; Raghavachari, K.; Pople, J. A. *J. Chem. Phys.* **2001**, *114*, 108–117.

(27) Montgomery, J. A., Jr.; Frisch, M. J.; Ochterski, J. W.; Petersson, G. A. *J. Chem. Phys.* **1999**, *110*, 2822–2827.

(28) Martin, J. M. L.; De Oliveira, G. J. *J. Chem. Phys.* **1999**, *111*, 1843–1856.

(29) Parthiban, S.; Martin, J. M. L. *J. Chem. Phys.* **2001**, *114*, 6014–6029.

(30) Scott, A. P.; Radom, L. *J. Phys. Chem.* **1996**, *100*, 16502–16513.

(31) Wong, M. W.; Radom, L. *J. Phys. Chem.* **1995**, *99*, 8582–8588.

(32) Wong, M. W.; Radom, L. *J. Phys. Chem. A* **1998**, *102*, 2237–2245.